

VACUUM PACKAGED MEMS PIEZOELECTRIC VIBRATION ENERGY HARVESTERS

R. Elfrink, M. Renaud, T. M. Kamel, C. de Nooijer, M. Jambunathan, M. Goedbloed, D. Hohlfeld, S. Matova, and R. van Schaijk

IMEC / Holst Centre, Eindhoven, The Netherlands

Abstract: This paper describes the characterization of thin film MEMS vibration energy harvesters based on aluminum nitride as piezoelectric material. A record output power of 85 μW has been measured. The parasitic damping contributions present in vacuum packaged and unpackaged energy harvesters are investigated. It is found that vacuum packaging of the harvester is essential for maximizing the output power. Therefore, a wafer-scale vacuum package process has been developed.

Keywords: piezoelectric, energy harvester, parasitic damping, vacuum package.

INTRODUCTION

This work describes the characterization of piezoelectric MEMS vibration energy harvesters [1] based on aluminum nitride and making use of a wafer level vacuum packaging. Aluminum nitride (AlN) was chosen as piezoelectric material for its material properties and its well-known sputter process. For power generation AlN is better or at least comparable with other piezoelectric materials like, e.g. PZT [2]. For the fabricated devices, the harvester effectiveness EH, as described in reference [3], equals 13%, which is comparable to different types of macroscopic harvesters.

Devices of different dimensions (table 1) were designed to cover a broad frequency range from 285 Hz to 1100 Hz. All devices have a beam thickness of $42 \pm 3 \mu\text{m}$. Process variation over the 6" silicon wafer has resulted in a frequency variation of about 8% between similar devices types. A record maximum power of 85 μW has been measured on unpackaged device of type 10 at an acceleration of 1.75 g and a resonance frequency of 325 Hz (figure 1).

We consider the package of MEMS harvesters to be essential for reliability as it prevents excessive mass displacements and protects the silicon beam from external influences. However, the package introduces additional parasitic damping due to squeeze film effect. For this reason, it is relevant to implement a vacuum packaging approach. The goal of this article is to investigate the influence of the package and pressure on the performances of MEMS harvesters.

We present measurements from devices with different dimension to show examples of our results; similar results were obtained for all devices types.

Table 1. Device types: length in mm and size in mm^2 .

Device type	1	3	5	7	9	10
Beam length	1.3	1.6	1.0	1.3	2.1	1.2
Mass size	3x3	3x3	5x5	5x5	7x7	7x7

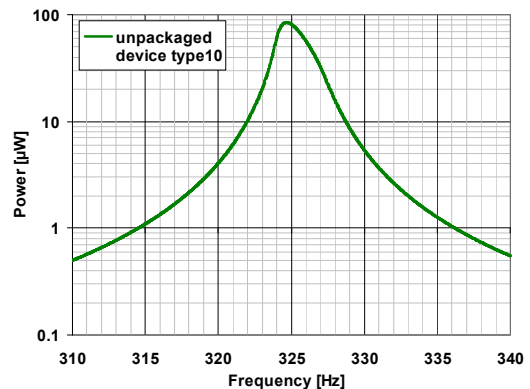


Fig. 1. An unpackaged device type 10 generates 85 μW at an excitation of 1.75 g at atmospheric pressure.

FABRICATION

The piezoelectric capacitor is formed by consecutive deposition, lithography and etching steps of the platinum bottom electrode, the AlN piezoelectric layer and the aluminum top electrode. The silicon mass and beam are shaped by subsequent front- and backside etching. Glass capping wafers with 400 μm deep cavities are etched with hydrofluoric acid and contact holes are realized with powder blasting.

The wafer-scale vacuum package process is shown in figure 2. A 1.0 μm thick SU-8 bonding layer is applied on the glass capping wafers. The roller-coating process applies the SU-8 film only on the elevated areas, the cavities and contact holes remain uncoated. The glass and silicon wafers are put under

vacuum conditions and bonded to each other by applying a temperature step which cures the SU-8. After dicing individual devices are obtained.

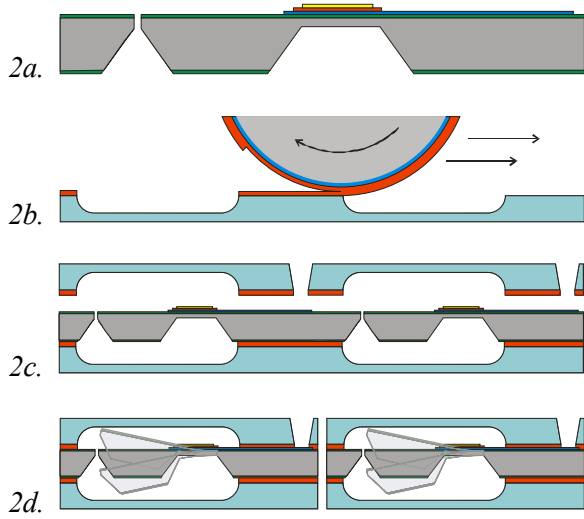


Fig. 2a-d. Process flow.

2a. The AlN piezoelectric capacitor is located on top of the beam. The Si mass and beam are fabricated by subsequent front- and backside etching.

2b. The SU-8 bonding layer is applied with a wafer scale roller-coating process on the glass wafers.

2c. The two glass wafers and the silicon wafer are vacuum bonded in two consecutive bonding steps.

2d. After dicing, single devices are obtained with the movable mass and beam in the vacuum cavity.

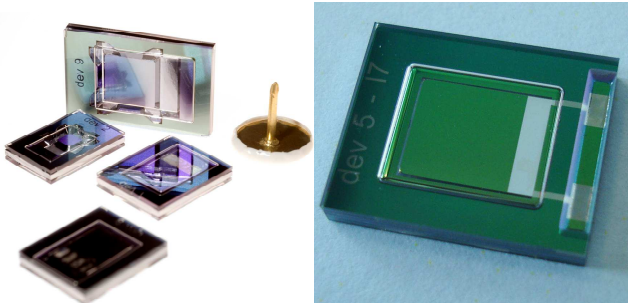


Fig. 3. Photograph of vacuum packaged vibration energy harvesters (left) and a close up (right) of a device showing the glass cap and contact openings.

DAMPING CONTRIBUTIONS

The vibration harvesters are represented as a dashpot mass-spring system [4] with three damping contributions to the quality factor: parasitic structural damping (Q_s), parasitic fluid damping (Q_f) and electrical damping (Q_e) due to the energy harvesting process.

The structural damping is related to thermoelastic losses occurring in the bulk of the material and to the radiation of elastic waves through the structural support of the vibrating beam [5]. Mechanical surface effects in the different layers of the piezoelectric capacitor can also add to the structural damping.

Fluid damping is related to the presence of a gas in the environment of the vibrating beam and mass. For pressure levels below 1 mbar the fluid damping mechanism corresponds to the collisions of the gas molecules with the oscillating parts of the structure (free molecular regime) [6]. Above 10 mbar the viscous damping force exerted by the ambient gas dominates the fluid parasitic dissipations (continuum regime). The effects happening in the middle range of pressure (1-10 mbar) correspond to the so-called transition regime. These effects are merely understood as a combination of the effects occurring in the free molecular and continuum regime.

Electrical damping is related to the conversion of kinetic energy of the moving mass into electricity. The consumed power in the electrical domain is equal to the power removed from the mechanical system and is considered as electrical induced damping.

In the case of packaged devices, the ambient gas is constrained by additional boundary conditions of the top and bottom capping plate of the package. As a result the fluidic damping is much larger due to the so called squeeze film effect [7].

The total quality factor Q_t of the described system can be expressed as given in (1).

$$\frac{1}{Q_t} = \frac{1}{Q_s} + \frac{1}{Q_f} + \frac{1}{Q_e} \quad (1)$$

We investigate in this paper the contribution of these different types of damping on our harvesters and their influence on the generated power.

QUANTIFICATION OF PARASITIC DAMPING

Measurements of the quality factors Q_s and Q_f related to parasitic damping were performed by measuring the frequency dependence of the open circuit voltage or the short circuit current ($Q_e \rightarrow \infty$) under different levels of pressure, for both packaged and unpackaged devices. A small opening was made in the glass top cover of packaged devices to enable control of the pressure inside the package.

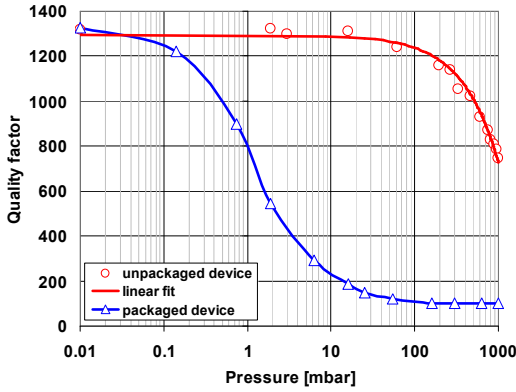


Fig. 4. The measured quality factors as a function of pressure. The unpacked device is hindered by viscous damping; the package device by squeeze film damping.

Figure 4 shows that for the unpacked device the fluid damping in the free molecular and transition regime does not have influence on the total quality factor. Therefore, the fluid damping has a smaller amplitude than the structural damping ($Q_s \ll Q_f$). The effect of fluid damping appears clearly in the continuum regime above 10 mbar. We observed a linear decrease of the measured quality factor with pressure. In this case, the parasitic dissipations are a combination of structural and fluid damping contributions. At 1000 mbar the fluid and structural damping are about equal ($Q_f \approx Q_s$).

The amplitude of the fluid damping is much larger for packaged devices, because of the before mentioned squeeze film effect. This parasitic damping mechanism overcomes the structural damping in all the different regimes and $Q_f \ll Q_s$ for pressure as low as 0.1 mbar. At atmospheric pressure the squeeze film effect dominates the parasitic dissipations.

When considering a vacuum packaging approach, it is recommended to reduce the pressure below 0.1 mbar in order to prevent the parasitic dissipations due to the squeeze film effect of fluid damping.

EFFECT OF PARASITIC DAMPING

Unpackaged devices

An unpackaged device of type 5 is excited at an input acceleration of 0.2 g at atmospheric pressure and at vacuum level (pressure < 0.1 mbar) where $Q_s \ll Q_f$. The resonance curves in figure 5 are measured at the optimum load resistance of 450 k Ω . The output power at atmospheric pressure is 1.46 μ W and in vacuum it is 6.9 μ W. The quality factors Q_t obtained from the resonance curves are 256 and 560 respectively. Furthermore, a shift of the resonance frequency from

596.8 Hz to 598.7 Hz is observed. The only changed variable here is the damping contribution of air to the vibrating mass. Therefore, at reduced damping, the mass displacement is larger, yielding a higher strain in the beam and thus generating more piezoelectric current through the load. As a result the power roughly quadrupled by preventing air damping.

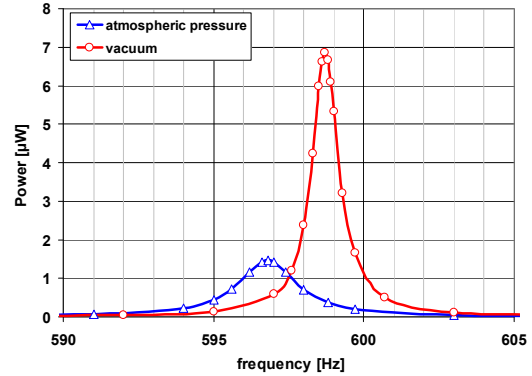


Fig. 5. Resonance curves of an unpacked device of type 5 at 0.2 g at atmospheric pressure and at vacuum showing an increase in power.

This measurement is repeated at short circuit current to prevent electrical damping both at atmospheric pressure and vacuum. The last obtained quality factor corresponds to the structural quality factor Q_s . All damping contributions to the quality factor could now be determined by using equation 3 and are summarized in table 2. One can conclude that for this example fluid damping is the major damping contribution.

Table 2. Quality factors for an unpacked device type 5 at 0.2 g.

Total quality factor		Quality factor	
$Q_t = Q_s$	996	Q_s	1000
$Q_t = Q_s // Q_f$	349	Q_f	500
$Q_t = Q_s // Q_e$	560	Q_e	1250
$Q_t = Q_s // Q_f // Q_e$	256		

Figure 6 shows the measured output power for the same device at 0.2 g at the resonance frequency as a function of pressure. One can deduce from the linear relation between mass displacement and current that the power is quadratic dependent of the quality factor, and thus pressure. Furthermore, the previously observed linear relation between the quality factor and pressure will also lead to a linear dependency of the resonance frequency and pressure. Both are confirmed in figure 6 by the good fit with a second order and linear function respectively. It is clear that at atmospheric pressure the power is about one quarter

of the value achieved at low pressure, where it seems to saturate to its maximum value.

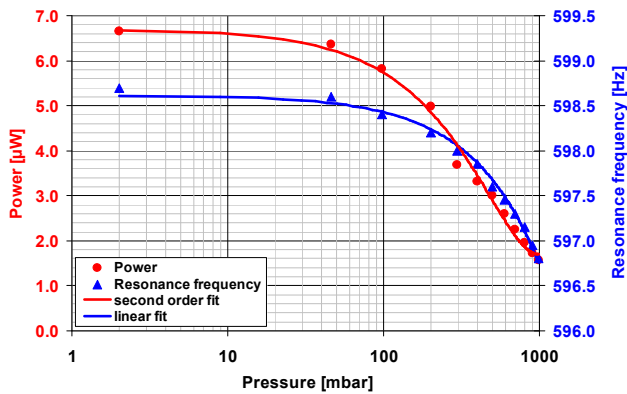


Fig. 6. Power and resonance frequency versus pressure for an unpackaged device of type 5 at an acceleration of 0.2 g.

Comparison of packaged and unpackaged devices

The output power of unpackaged, atmospheric packaged and vacuum packaged devices of type 3 has been measured and modeled [8, 9] as a function of acceleration, figure 7.

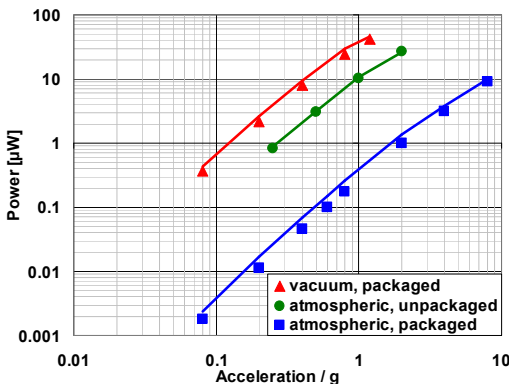


Fig. 7. Measured (dots) and modeled (lines) power as function of acceleration for a device type 3. The highest power is generated with a vacuum package.

It is obvious that the atmospherically packaged harvester generates the lowest output power. This is explained by the effect of squeeze film damping. Higher power is measured with the unpackaged devices, since here viscous air damping without squeeze film effects is present. The highest power output is measured with vacuum packaged devices, where parasitic damping is limited to the structural component. The results are compared at 1.0 g (using interpolation of the measured data) in table 3.

Table 3. The output power and quality factor at 1.0 g of device type 3 with different packaging.

	Power [μ W]	Q_t
Atmospheric package	0.27	80
Unpackaged	10.2	430
Vacuum package	32.0	810

Due to the absence of air damping the increase in quality factor is about ten fold and the resulting increase in power output is about hundred fold.

The used model calculates the generated charge caused by the strain in the piezoelectric layer due to the bending of the silicon beam during vibration. A good agreement between measurements and modeled results is obtained.

CONCLUSION

A record power for a MEMS type vibration energy harvester of 85 μ W is measured at 1.75 g.

We could successfully determine contributions of different damping mechanisms by considering the harvester as damped mass-spring system.

With the developed wafer-scale vacuum package process we were able to achieve higher power at lower acceleration. Parasitic fluid damping was completely prevented by pressures below 0.1 mbar.

REFERENCES

- [1] S.P. Beeby et al., *Meas. Sci. Technol.* 17, R175, 2006
- [2] R. Elfrink et al., *J. Micromech. Microeng.* 19 (2009) 094005
- [3] P.D. Mitcheson et al., *J. Micromech. Microeng.* 17, S211, 2007
- [4] S. Roundy et al., *Energy scavenging for wireless sensor networks*, Kluwer Academic Publishers, ISBN 1-4020-7663-0, 2004
- [5] T. V. Roszart, *Proc. IEEE Solid-State Sensor and Actuator Workshop*, 1990, pp. 13–16.
- [6] Z. Weibin, K. L. Turner, *Proc IEEE Sensors 2005*
- [7] H. Noura et al., *J. of Sound and Vibration* 305, 243–260, 2007
- [8] M. Renaud et al., *Sensors and Actuators A* 145–146, pp.380, 2008
- [9] S. Matova et al., *Euroensors 2008*, p1482–p1485.